Surface Science 603 (2009) 683–689

Contents lists available at ScienceDirect

Surface Science

journal homepage: www.elsevier.com/locate/susc

Fractional statistical theory and use of quasi-chemical approximation for adsorption of interacting *k*-mers

M. Dávila, J.L. Riccardo, A.J. Ramirez-Pastor *

Dpto. de Física, Instituto de Física Aplicada, Universidad Nacional de San Luis – CONICET, Chacabuco 917, 5700 San Luis, Argentina

ARTICLE INFO

Article history:
Received 7 October 2008
Accepted for publication 23 December 2008
Available online 14 January 2009

Keywords:
Lattice-gas models
Multisite occupancy
Adsorption isotherms

ABSTRACT

In a recent paper [J.L. Riccardo, A. J. Ramirez-Pastor, F. Romá, Phys. Rev. Lett. 94 (2004) 186101], a new fractional statistical theory of adsorption (FSTA) based on Haldane's statistics was presented. Later [M. Dávila, F. Romá, J.L. Riccardo, A.J. Ramirez-Pastor, Surf. Sci. 600 (2006) 2011], a generalization of the classical quasi-chemical approximation (QCA) was developed in which the adsorbate can occupy more than one adsorption site. In this paper, we describe the statistical thermodynamics of interacting polyatomic adsorbates (*k*-mers) on homogeneous surfaces, by combining FSTA and QCA. The main thermodynamic functions are obtained in terms of two parameters, *g* and *a*, which are related directly to the spatial configuration of a polyatomic molecule in the adsorbed state. Analysis of simulated and experimental results have been carried out in order to (i) explore the reach and limitations of the theoretical model and (ii) evince the physical significance of *g* and *a*.

1. Introduction

The theoretical description of adsorption of polyatomic molecules of arbitrary shape and size is a current and exciting topic of research in surface science [1–5]. Adsorption experiments in the laboratory and applications involve species larger than monoatomics. To practical purposes, the deeper our knowledge of the influence of the various factors affecting adsorption, the better our accuracy to characterize the surface and to design specific-purposes adsorbents. The drawback in treating lattice gases of polyatomic species within the framework of statistical mechanics is to properly calculate the configurational entropy. Configuration counting in the case of particles that occupy more than one lattice site (dimers, trimers, etc.), seems a hopeless task, and it limits the analytical developments in the field of adsorbed polyatomic gases.

Quantum fractional statistics (QFS) proposed by Haldane [6] and Wu [7], based upon a generalization of the Pauli's exclusion principle, is a theoretical frame that allows us to rationalize the site-exclusion effect that results from the multisite occupancy as "statistical interactions" characterized by a parameter *g*; this parameter essentially accounts for the number of states (out of the states available to a single particle) that a particle excludes when adsorbed on the surface. Formally speaking, in quantum mechanics, fermions and bosons correspond to $g = 1$ and $g = 0$, respectively. However, particles obeying fractional statistics exist, for which $0 < g < 1$. In recent work [8–10], we extended these ideas and presented the basis of a fractional statistics thermodynamic theory of adsorption (FSTA) of polyatomics as to describe the thermodynamic properties of the adlayer when the adsorbate occupies more than one adsorption site. The treatment of this complex problem can be significantly simplified if looked at from this perspective. In this case the parameter *g* varies within the interval $g > 1$.

In our previous work we assumed that the molecules do not interact each other but only interact with the substrate through an adsorption energy per particle ϵ_0 (that depends on the molecular species), adsorbate–adsorbate interactions, however, play an important role in determining the main properties for many adsorbed systems [11–19].

In the present paper, we introduce the contribution of interactions between molecules to the free energy obtained from FSTA, through a quasi-chemical approximation (QCA) generalized to structured adsorbates [20,21]. The new theoretical framework provides a close approximation for two-dimensional systems accounting multisite occupancy and lateral interactions between admolecules.

The present work is organized as follows. In Section 2, we provide the theoretical formalism and derive the analytical form of the main thermodynamic functions. The results of the theoretical approach are presented in Section 3, along with a comparison with Monte Carlo simulation and experimental data. Finally, the conclusions are drawn in Section 4.

2. Basic formalism: thermodynamic functions

We consider the general case of adsorbates containing *k* identical units, each of one occupying a lattice site. Small adsorbates

* Corresponding author. Fax: +54 2652 430224.
E-mail address: antorami@unsl.edu.ar (A.J. Ramirez-Pastor).

0039-6028/$ - see front matter © 2009 Elsevier B.V. All rights reserved.
doi:10.1016/j.susc.2008.12.032

with spherical symmetry would correspond to the monomer limit ($k = 1$). The distance between k-mer units is assumed in registry with the lattice constant; hence exactly k sites are occupied by a k-mer when adsorbed. Two different energies are considered in the adsorption process: (1) U_0, constant interaction energy between a k-mer unit and an adsorption site and (2) w, lateral interaction energy between two nearest-neighbor units belonging to different k-mers. Then, the canonical partition function can be written as [20]:

$$Q(N,M,T) = q^N \sum_{N_{11}} \Omega(N,M,N_{11}) \exp[-\beta(wN_{11} + kNU_0)], \tag{1}$$

where q is the partition function for a single adsorbed molecule; M and N represent the number of adsorption sites and adsorbed k-mers, respectively; N_{11} is the number of pairs of nearest-neighbor units belonging to different k-mers; $\Omega(N,M,N_{11})$ is the number of ways to array N k-mers on M sites with N_{11} pair of occupied sites and $\beta = 1/k_BT$, being k_B the Boltzmann constant.

As it is usual in the case of single-site occupation, it is convenient to write the canonical partition function as a function of N_{01}, where N_{01} is the number of pairs formed by an empty site adjacent to a occupied site. For this purpose, we calculate the relations between N_{11}, N_{01} and N_{00} (N_{00} is the number of pairs of empty nearest-neighbor sites):

$$2N_{11} + N_{01} + 2N(k-1) = ckN, \tag{2}$$

$$2N_{00} + N_{01} = c(M - kN), \tag{3}$$

where "number of 01 pairs" = "number of 10 pairs" = $N_{01}/2$ and c is the coordination number of the lattice. In the case of $k = 1$, the well-known relations for single-site occupation are recovered [20].

Now, the canonical partition function can be written in terms of N_{01}

$$Q(N,M,T) = q^N \exp\{-\beta N[\lambda w/2 + kU_0]\} \sum_{N_{01}} \Omega(N,M,N_{01}) \times \exp(\beta w N_{01}/2) \tag{4}$$

and $\lambda = (c-2)k + 2$.

By using the standard formalism of the QCA, the number of ways of assigning a total of $[cM/2 - N(k-1)]$ independent pairs[1] to the four categories 11, 10, 01, and 00, with any number 0 through $[cM/2 - N(k-1)]$ per category consistent with the total, is

$$\widetilde{\Omega}(N,M,N_{01}) = \frac{[cM/2 - N(k-1)]!}{[(N_{01}/2)!]^2 [c(M-kN)/2 - N_{01}/2]! [\lambda N/2 - N_{01}/2]!}. \tag{5}$$

This cannot be set equal to $\Omega(N,M,N_{01})$ in Eq. (4), because treating the pairs as independent entities leads to some unphysical configurations (see Ref. [20, p. 253]). Thus $\widetilde{\Omega}$ overcounts the number of configurations. To take care of this, we must normalize $\widetilde{\Omega}$:

$$\Omega(N,M,N_{01}) = C(N,M)\widetilde{\Omega}(N,M,N_{01}) \tag{6}$$

and

$$\Omega(N,M) = \sum_{N_{01}} \Omega(N,M,N_{01}) = C(N,M) \sum_{N_{01}} \widetilde{\Omega}(N,M,N_{01}), \tag{7}$$

where $\Omega(N,M)$ is the number of ways to arrange N k-mers on M sites. In general, $\Omega(N,M)$ depends on the spatial configuration of the k-mer and the surface geometry. Even in the simplest case of linear k-mers, there not exist the exact form of $\Omega(N,M)$ in two (or more) dimensions. However, different approximations have been developed for $\Omega(N,M)$ [22,23], which allow us to obtain $C(N,M)$.

[1] The term $N(k-1)$ is subtracted since the total number of nearest-neighbor pairs, $cM/2$, includes the $N(k-1)$ bonds belonging to the N adsorbed k-mers.

In order to calculate $C(N,M)$, we replace $\sum_{N_{01}} \widetilde{\Omega}(N,M,N_{01})$ by the maximum term in the sum, $\widetilde{\Omega}(N,M,N_{01}^*)$. By taking logarithm of Eq. (5), and using the Stirling's approximation we obtain:

$$\begin{aligned}\ln \widetilde{\Omega}(N,M,N_{01}) = {} & [cM/2 - (k-1)N] \ln[cM/2 - (k-1)N] \\ & - N_{01} \ln N_{01}/2 - [c(M-kN)/2 - N_{01}/2] \\ & \times \ln[c(M-kN)/2 - N_{01}/2] - (\lambda N/2 \\ & - N_{01}/2) \ln(\lambda N/2 - N_{01}/2).\end{aligned} \tag{8}$$

Differentiating the last equation with respect to N_{01} yields

$$\widetilde{\Omega}'(N,M,N_{01}) = \frac{\widetilde{\Omega}(N,M,N_{01})}{2} \ln\left\{\frac{[c(M-kN) - N_{01}](\lambda N - N_{01})}{N_{01}^2}\right\}. \tag{9}$$

Setting $\widetilde{\Omega}'(N,M,N_{01}) = 0$ and solving for N_{01}^*, the value of N_{01} in the maximum term of $\widetilde{\Omega}$,

$$N_{01}^* = \frac{c\lambda N(M-kN)}{cM - 2(k-1)N} = \lambda N - \frac{\lambda^2 N^2}{cB}, \tag{10}$$

and

$$B = M - 2(k-1)N/c. \tag{11}$$

Then,

$$\widetilde{\Omega}(N,M,N_{01}^*) = \frac{(cB/2)!}{\left[\left(\lambda N/2 - \frac{\lambda^2 N^2}{2cB}\right)!\right]^2 \left(cB/2 - \lambda N + \frac{\lambda^2 N^2}{2cB}\right)! \left(\frac{\lambda^2 N^2}{2cB}\right)!}, \tag{12}$$

and, by simple algebra,

$$\widetilde{\Omega}(N,M,N_{01}^*) = \left[\frac{B!}{(B - \lambda N/c)!(\lambda N/c)!}\right]^c. \tag{13}$$

Eq. (13) allows us to calculate $C(N,M)$,

$$C(N,M) = \frac{\Omega(N,M)}{\widetilde{\Omega}(N,M,N_{01}^*)} = \Omega(N,M)\left[\frac{(B - \lambda N/c)!(\lambda N/c)!}{B!}\right]^c. \tag{14}$$

Now, $\ln Q(N,M,T)$ [see Eq. (4)] can be written as

$$\ln Q(N,M,T) = N \ln q - \beta N[\lambda w/2 + kU_0] + \ln\left\{\sum_{N_{01}} C(N,M)\widetilde{\Omega}(N,M,N_{01}) \exp(\beta w N_{01}/2)\right\}. \tag{15}$$

As in Eq. (7), we replace $\sum_{N_{01}} C(N,M)\widetilde{\Omega}(N,M,N_{01}) \exp(\beta w N_{01}/2)$ by the maximum term in the sum, $C(N,M)\widetilde{\Omega}(N,M,N_{01}^{**}) \exp(\beta w N_{01}^{**}/2)$. Thus,

$$C(N,M)\widetilde{\Omega}'(N,M,N_{01}^{**}) \exp(\beta w N_{01}^{**}/2) + C(N,M)\widetilde{\Omega}(N,M,N_{01}^{**}) \exp(\beta w N_{01}^{**}/2)\beta w/2 = 0, \tag{16}$$

then,

$$\frac{\widetilde{\Omega}'(N,M,N_{01}^{**})}{\widetilde{\Omega}(N,M,N_{01}^{**})} = -\beta w/2. \tag{17}$$

From Eqs. (9) and (17),

$$(cB - \lambda N - N_{01}^{**})(\lambda N - N_{01}^{**}) = {N_{01}^{**}}^2 \exp(-\beta w) \tag{18}$$

and

$$[1 - \exp(-\beta w)]{N_{01}^{**}}^2 - cBN_{01}^{**} + (cB - \lambda N)\lambda N = 0. \tag{19}$$

Solving Eq. (19) we obtain

$$\frac{N_{01}^{**}}{cB} = \frac{1 - \sqrt{1 - 4A(1 - \lambda N/cB)(\lambda N/cB)}}{2A}. \tag{20}$$

where $A = 1 - \exp(-\beta w)$. The solution $N_{01}^{**}/cB = (1 + \sqrt{\cdots})/2A$ is discarded for physical grounds.[2]

Finally, the canonical partition function can be written in terms of N_{01}^{**},

$$Q(N,M,T) = q^N \exp\{-\beta N[\lambda w/2 + kU_0]\}\Omega(N,M) \times \left[\frac{(B-\lambda N/c)!(\lambda N/c)!}{B!}\right]^c \widetilde{\Omega}(N,M,N_{01}^{**}) \exp(\beta w N_{01}^{**}/2) \quad (21)$$

Taking logarithm and using the Stirling's approximation yields:

$$\begin{aligned}\ln Q(N,M,T) = {} & N\ln q - \beta N[\lambda w/2 + kU_0] + \beta w N_{01}^{**}/2 + \lambda N \\ & \times \ln \lambda N/c - cB\ln B + (cB/2)\ln(cB/2) - N_{01}^{**} \\ & \times \ln N_{01}^{**}/2 + c(B-\lambda N/c)\ln(B-\lambda N/c) \\ & - (cB/2 - \lambda N/2 - N_{01}^{**}/2)\ln(cB/2 - \lambda N/2 \\ & - N_{01}^{**}/2) - (\lambda N/2 - N_{01}^{**}/2)\ln(\lambda N/2 \\ & - N_{01}^{**}/2) + \ln\Omega(N,M). \end{aligned} \quad (22)$$

The Helmholtz free energy per site, $f(N,M,T) = F(N,M,T)/M[\beta F(N,M,T) = -\ln Q(N,M,T)]$, can be obtained from Eq. (22), as a function of surface coverage, $\theta = kN/M$, and temperature,

$$\begin{aligned}\beta f(\theta,T) = {} & -\frac{\theta}{k}\ln q + \beta\frac{\theta}{k}\left(\frac{\lambda w}{2} + kU_0\right) - \lambda\frac{\theta}{k}\ln\frac{\lambda\theta}{ck} \\ & + \left[c - 2\left(\frac{k-1}{k}\right)\theta\right]\ln\left[1 - \frac{2}{c}\left(\frac{k-1}{k}\right)\theta\right] \\ & - \left[\frac{c}{2} - \left(\frac{k-1}{k}\right)\theta\right]\ln\left[\frac{c}{2} - \left(\frac{k-1}{k}\right)\theta\right] + \frac{\lambda\theta}{2k}\ln\left(\frac{\lambda\theta}{2k} - \alpha\right) \\ & - c\left[1 - \frac{2}{c}\left(\frac{k-1}{k}\right)\theta - \frac{\lambda\theta}{ck}\right]\ln\left[1 - \frac{2}{c}\left(\frac{k-1}{k}\right)\theta - \frac{\lambda\theta}{ck}\right] \\ & + \left[\frac{c}{2} - \left(\frac{k-1}{k}\right)\theta - \frac{\lambda\theta}{2k}\right]\ln\left[\frac{c}{2} - \left(\frac{k-1}{k}\right)\theta - \frac{\lambda\theta}{2k} - \alpha\right] - \ln\gamma \end{aligned} \quad (23)$$

where α is

$$\alpha = \frac{N_{01}^{**}}{2M} = \frac{\lambda c}{2k}\frac{\theta(1-\theta)}{\left[\frac{c}{2} - \left(\frac{k-1}{k}\right)\theta + b\right]}, \quad (24)$$

$$b = \left\{\left[\frac{c}{2} - \left(\frac{k-1}{k}\right)\theta\right]^2 - \frac{\lambda c}{k}A\theta(1-\theta)\right\}^{1/2} \quad (25)$$

and

$$\gamma = \Omega(N,M)^{1/M}. \quad (26)$$

The equilibrium properties of the adlayer can be obtained from Eq. (22) along with the differential form of F in the canonical ensemble

$$dF = -SdT - \Pi dM + \mu dN \quad (27)$$

where S, Π and μ represent the entropy, the spreading pressure and the chemical potential, respectively.

Thus, the coverage dependence of the chemical potential, $\mu[= (\partial F/\partial N)_{M,T}]$, arises straightforwardly from Eqs. (22) and (27)

$$\begin{aligned}\beta\mu = {} & -\ln K(T) + \frac{\beta\lambda w}{2} - \lambda\ln\frac{\lambda\theta}{ck} - 2(k-1)\ln\left(1 - \frac{2\theta}{c} + \frac{2\theta}{ck}\right) \\ & + (k-1)\ln\left(\frac{c}{2} - \theta + \frac{\theta}{k}\right) + ck\ln(1-\theta) - \frac{ck}{2} \\ & \times \ln\left[\frac{c}{2}(1-\theta) - \alpha\right] + \frac{\lambda}{2}\ln\left(\frac{\lambda\theta}{2k} - \alpha\right) - k\frac{\partial\ln\gamma}{\partial\theta}, \end{aligned} \quad (28)$$

where $K(T) = q\exp(-\beta k U_0)$ is the equilibrium constant.

In this point, it is important to emphasize the main differences between the results obtained in previous work [21] and the corresponding ones in the present paper. In Ref. [21], a theory for adsorption of interacting polyatomic molecules based on the well-known QCA [20] was presented. The approach was obtained by combining (i) the exact analytical expression for the partition function of non-interacting linear k-mers adsorbed in one dimension and its extension to higher dimensions, and (ii) a generalization of the classical QCA in which the adsorbate can occupy more than one adsorption site. In this paper, we allow for the introduction of any of the configurational factors associated to adsorption of non-interacting k-mers (Flory–Huggins factor [24,25], Guggenheim–DiMarzio factor [26,27], FSTA factor [8], semiempirical factor [22], etc.). Accordingly, the main thermodynamic functions are now explicitly written in terms of Ω (or γ). This modification can be better understood by comparing Eqs. (23) and (28) of the present manuscript with Eqs. (25) and (29) of Ref. [21]. The new theoretical scheme allows us to deal with adsorbates of arbitrary shape and size, beyond of the rigid linear molecules studied in Ref. [21].

As it was discussed in Section 1, we are interested in obtaining a theoretical description in the framework of the fractional statistics. For this purpose, the function γ will be calculated from FSTA.

In the following, we summarize the basis of the FSTA description [8], which allows to describe the configurational entropy through a single function (parameter), namely the statistical exclusion, g, accounting for the configuration of the molecules in the adsorbed state. In this approximation, the interaction of one isolated molecule with a solid surface confined in a fixed volume is represented by an adsorption field having a total number G of local minima in the coordinate space necessary to define the adsorption configuration. Thus, G is the number of equilibrium states of a single molecule at infinitely low density. In general, more than one state out of G are prevented from occupation upon adsorption of a molecule. Furthermore, because of possible concurrent exclusion of states by two or more molecules, the number of states excluded per molecule, $g(N)$, being a measure of the "statistical" interactions, depends in general on the number of molecules N within the volume. From the definition of the number of states available for a Nth molecule after $(N-1)$ ones are already in the volume V, $d_N = G - \sum_{N'=1}^{N-1} g(N') = G - G_0(N)$, a generalization of the expression introduced by Haldane [6], the generalized configurational factor, $\Omega(N,G) = (d_N + N - 1)!/[N!(d_N - 1)!]$, can be calculated. Consequently,

$$\frac{\partial\ln\Omega^*}{\partial n} = \ln\left\{\frac{[1-\widetilde{G}_0(n)]^{\widetilde{G}_0'}}{n[1-\widetilde{G}_0(n)+n]^{(\widetilde{G}_0'-1)}}\right\}, \quad (29)$$

where $n = N/G$ is the density (n finite as $N,G\to\infty$), $\Omega^* \equiv \lim_{N,G\to\infty}\Omega(N,G)^{1/G}$, $\widetilde{G}_0(n) \equiv \lim_{N,G\to\infty} G_0(N)/G$ and $\widetilde{G}_0' \equiv d\widetilde{G}_0/dn$.

Furthermore, by taking the simplest approximation within FSTA, namely $g = $ constant ($\widetilde{G}_0(n) = gn$ and $\widetilde{G}_0' = g$), a particular function arises from Eq. (29)

$$\ln\left[\frac{[1-\widetilde{G}_0(n)]^{\widetilde{G}_0'}}{n[1-\widetilde{G}_0(n)+n]^{(\widetilde{G}_0'-1)}}\right] = \ln\left\{\frac{[1-a\theta g]^g}{a\theta[1-a\theta(g-1)]^{g-1}}\right\} \quad (30)$$

$n = a\theta$, θ being either the ratio N/N_m or the ratio v/v_m, where $N(v)$ is the number of adsorbed molecules (adsorbed amount) at given (μ,T) and $N_m(v_m)$ is the one corresponding to monolayer completion.

For molecules constituted by k identical units, each of which can occupy an adsorption site, $N_m = M/k$, $\theta = kN/M$ (as it was defined above) and $G = mM$, where $m(\equiv m(c,k))$ is the number of distinguishable configurations of the molecule per lattice site (at zero

[2] If the positive sign is chosen in solving Eq. (19), N_{01}^{**} becomes negative for attractive interactions ($A < 0$) and larger than $cB/2$ for repulsive interactions ($0 < A < 1$).

density) and depends on the lattice/molecule geometry. Then, from Eqs. (29) and (30),

$$k\frac{\partial \ln \gamma}{\partial \theta} = \ln\left\{\frac{[1-a\theta g]^g}{a\theta[1-a\theta(g-1)]^{g-1}}\right\}. \tag{31}$$

Replacing Eq. (31) in Eq. (28), a new adsorption isotherm is obtained, which combines FSTA and QCA.

The parameters a and g in the last equation have a precise physical meaning and can be obtained from adsorption experiments. They are related directly to the spatial configuration of a polyatomic molecule in the adsorbed state. Alternatively, Eq. (31) can be used assuming some approach to calculate a and g as a function of the model's parameters. Thus, given shape and size of adsorbate, the adsorption isotherm is straightforwardly obtained. In the next section, Eq. (31) will be used in both ways.

3. Results

In a first stage, MC simulations were used in order to test the applicability of the new theoretical approach. The system chosen for the comparison was a lattice-gas of interacting dimers,[3] whose Hamiltonian can be written as:

$$H = w\sum_{\langle i,j\rangle} c_i c_j - Nw + U_o\sum_i c_i, \tag{32}$$

where $\langle i,j\rangle$ represents pairs of nearest-neighbor sites and c_i is the occupation variable, which can take the following values: $c_i = 0$ if the corresponding site is empty and $c_i = 1$ if the site is occupied. The term Nw is subtracted in Eq. (32) since the summation over all the pairs of nearest-neighbor sites overestimates the total energy by including N bonds belonging to the N adsorbed dimers. In the simulations, U_o is set equal zero, without any lost of generality.

The adsorption process is simulated through a grand canonical ensemble Monte Carlo (GCEMC) method [28–30]. For a given value of the temperature T and chemical potential μ, an initial configuration with N dimers adsorbed at random positions (on $2N$ sites) is generated. Then an adsorption–desorption process is started, where a pair of nearest-neighbor sites is chosen at random and an attempt is made to change its occupancy state with probability given by the Metropolis rule [31]:

$$P = \min\{1, \exp(-\beta\Delta H)\} \tag{33}$$

where $\Delta H = H_f - H_i$ is the difference between the Hamiltonians of the final and initial states. A Monte Carlo step (MCS) is achieved when M pair of sites have been tested to change their occupancy state. The equilibrium state can be well reproduced after discarding the first $m\prime = 10^5 - 10^6$ MCS. Then, averages are taken over $m = 10^5 - 10^6$ successive configurations. The mean coverage θ is obtained as simple average:

$$\theta = \frac{1}{M}\sum_i^M \langle c_i\rangle = 2\frac{\langle N\rangle}{M} \tag{34}$$

where $\langle N\rangle$ is the mean number of adsorbed particles and $\langle\cdots\rangle$ means the time average over the Monte Carlo simulation runs.

The computational simulations have been developed for honeycomb, square and triangular $L\times L$ lattices, with $L = 144$, 144 and 150, respectively, and periodic boundary conditions. With these lattice sizes we verified that finite-size effects are negligible. Note, however, that the linear dimension L has to be properly chosen such that the adlayer structure is not perturbed.[4] All calculations were carried out using the BACO parallel cluster (composed by 60 PCs each with a 3.0 GHz Pentium-4 processor) located at Laboratorio de Ciencias de Superficies y Medios Porosos, Universidad Nacional de San Luis, San Luis, Argentina.

In order to evince the physical significance of a, we write this parameter as[5] $a = (km)^{-1}$, where m is the number of distinguishable configurations of the molecule per lattice site at zero density. $m(c,k)$ is, in general, a function of the connectivity and the size of the adsorbate. It is easy to show that,

$$m(c,k) = \begin{cases} c/2 & \text{for rigid } k\text{-mers} \\ [c(c-1)^{(k-2)}]/2 - m' & \text{for flexible } k\text{-mers} \end{cases} \tag{35}$$

the term m' is subtracted in Eq. (35) because the first term overestimates $m(c,k)$ by including m' configurations providing overlaps in the k-mer.

On the other hand, a relates to the low-density limit $(\theta\to 0), \beta\mu \approx \ln a\theta - \ln K(T)$, where $K(T) = q\exp(-\beta k U_0)$. Fig. 1 shows $\ln\theta$ vs. $\beta\mu$ for dimers adsorbed at low coverage on honeycomb, square and triangular lattices. Symbols and lines corresponding to results obtained from MC simulations and theory [Eqs. (28), (31) and (35)], respectively. The agreement between theoretical curves and simulation data supports the results given by Eq. (35). In addition, given that the effect of lateral interactions is negligible in the low-density limit, the results in Fig. 1 do not depend on w.

The study above allows us to calculate a from the spatial configuration of the adsorbed molecule at low density. Then, given the shape (and size) of the adsorbate and the surface geometry, the theoretical adsorption isotherm can be written in terms of an unique parameter g. By following this line of reasoning, simulated adsorption isotherms of interacting dimers on two-dimensional lattices were examined in terms of the new isotherm function. In our analysis, the parameter g was obtained in two different ways. Namely, (1) by fitting the simulation data; and (2) by assuming a simple approximation of adsorption site independence (AASI). Under this consideration, if one molecule has m different ways of adsorbing on one site, $g = mk$ states are excluded when one k-mer is adsorbed occupying k sites on the lattice.

Fig. 2 presents the adsorption isotherms for dimers on square lattices with different repulsive [part (a)] and attractive [part (b)] values of the lateral interaction energy. Symbols represent simulation results and lines correspond to theory. In the theoretical equations [Eqs. (28) and (31)], we fix $k = 2, c = 4, a = 1/4$ and set βw according to the computational data. With respect to g, solid and dashed lines correspond to curves calculated by using a value of the exclusion parameter obtained from the best fit to the numerical data and by assuming AASI, respectively. A similar study was also done for honeycomb and triangular lattices (data not shown here for brevity). The values of the parameters used in the adjustments are collected in Table 1.

The system presents different behavior according to the sign of the lateral interaction energy. For repulsive interactions [part (a) in Fig. 2], two well-defined and pronounced structures appear in the adsorbate (steps in the isotherms) at coverage $\theta_1 = 1/2$ and $\theta_2 = 2/3$. For $\theta = 1/2$ [2/3], a (4×2) ordered phase [a "zigzag" (ZZ) ordered phase], characterized by alternating files of dimers

[3] The dimer is the simplest case of a polyatomic adsorbate and contains all the properties of the multisite-occupancy adsorption.

[4] As it has been reported in the literature [15,16], two low-temperature ordered phases appear at coverage $\theta_1 = 5/9$ and $\theta_2 = 2/3$ for repulsive dimers on honeycomb lattices, $\theta_1 = 1/2$ and $\theta_2 = 2/3$ for square lattices and $\theta_1 = 2/5$ and $\theta_2 = 2/3$ for triangular lattices. Thus, in order to allow the formation of the ordered structures in the adlayer, the number of sites in each direction L is required to be a multiple of 9, 6 and 15 for honeycomb, square and triangular lattices, respectively.

[5] Note that $n = N/G, n = a\theta, \theta = kN/M$ and $G = mM$. Then, $a = (km)^{-1}$.

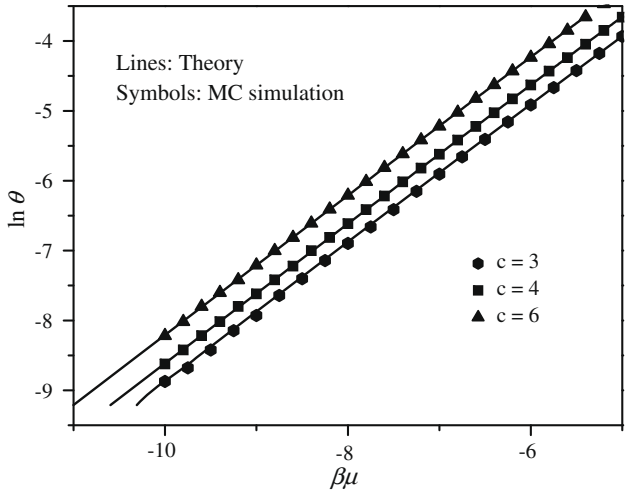

Fig. 1. $\ln\theta$ vs. $\beta\mu$ for dimers adsorbed at low coverage on honeycomb, square and triangular lattices. The symbols are indicated in the figure.

separated by 2 adjacent empty sites [characterized by domains of parallel ZZ strips oriented at ±45° from the lattice symmetry axes], is separated from the disordered state by a order–disorder phase transition occurring at a finite critical temperature [17,18]. The locations of the ordered phases depend on the geometry of the substrate, being $\theta_1 = 5/9$ and $\theta_2 = 2/3$ for honeycomb lattices, and $\theta_1 = 2/5$ and $\theta_2 = 2/3$ for triangular lattices [16].

For attractive interactions [part (b) in Fig. 2], adsorption isotherms shift to lower values of chemical potential and their slopes increase as βw increases. For temperatures below the critical value, the adlayer undergoes a first-order phase transition (with a clustering of the ad-particles), which is visualized as a clear discontinuity in the simulation isotherms and as a loop in the theoretical isotherms. In this situation, which has been observed experimentally in numerous systems [32,33], the only phase which one expects is a lattice-gas phase at low coverage, separated by a two-phase coexistence region from a "lattice-fluid" phase at higher coverage. The lattice-fluid can be considered as a version of the registered (1×1) phase (where every available site of the lattice is occupied) diluted with vacancies. This condensation of a two-dimensional gas to a two-dimensional liquid is similar to that of a lattice-gas of attractive monomers [20]. However, the symmetry particle-vacancy (valid for monoatomic particles) is broken for k-mers and the isotherms are asymmetric with respect to $\theta = 0.5$.

On the other hand, the critical value at which the condensation occurs, βw_c, depends on the structure of the lattice, being approximately 3, 1.5 and 1, for honeycomb, square and triangular lattices, respectively [15,16]. A simple explanation for this behavior is the following: to take a dimer out of a (1×1) structure and to destroy the island in the adsorbate, one needs an energy equivalent to $2(c-1)w$. For this reason, the structure is energetically more stable as c increases, so βw_c is shifted to lower values.

To complete the description of Fig. 2, the insets in parts (a) and (b) show a comparison between MC simulation (symbols), the present theory with fitted g (solid line) and a typical mean-field approximation (MFA) (dotted line), for two limit cases [$\beta w = 4$ in part (a) and $\beta w = -1$ in part (b)]. In the framework of MFA, the adsorption isotherm takes the form [34],

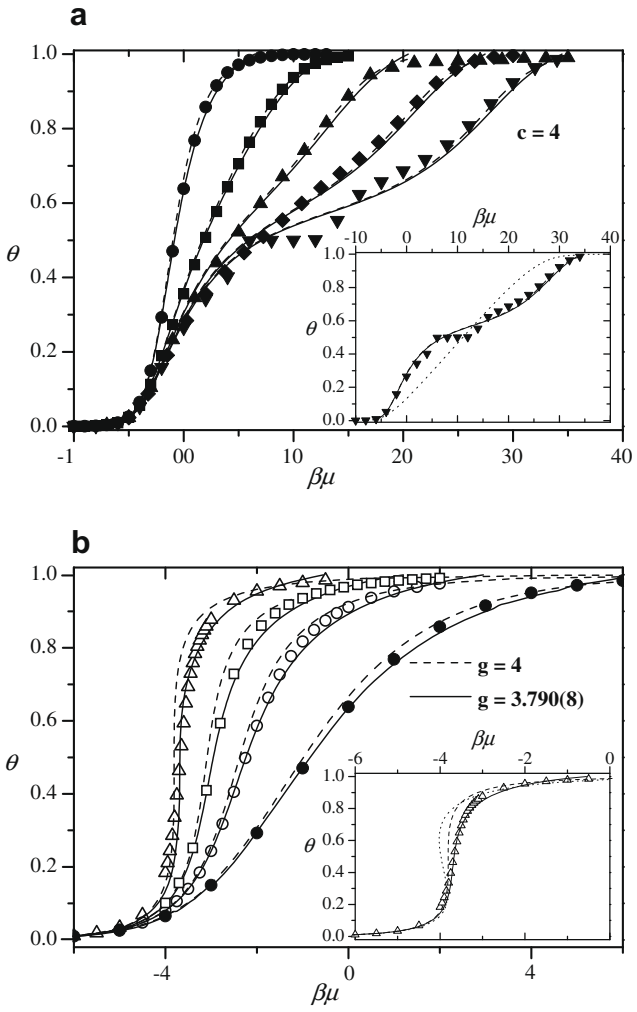

Fig. 2. Adsorption isotherms for homonuclear dimers adsorbed on a square lattice with nearest-neighbor interactions. Symbols represent Monte Carlo simulations. Solid and dashed lines correspond to theoretical results as explained in the text. Part (a) repulsive case: full circles, $\beta w = 0$; full squares, $\beta w = 1.0$; full up triangles, $\beta w = 2.0$; full diamonds, $\beta w = 3.0$ and full down triangles, $\beta w = 4.0$. Inset: Comparison between MC simulation (symbols), the present theory with fitted g (solid line) and MFA (dotted line) for $\beta w = 4.0$. Part (b) attractive case: full circles, $\beta w = 0$; open circles, $\beta w = -0.5$; open squares, $\beta w = -0.75$ and open up triangles, $\beta w = -1.0$. Inset: comparison between MC simulation (symbols), the present theory with fitted g (solid line) and MFA (dotted line) for $\beta w = -1.0$.

$$\beta\mu = -\ln q - \ln\frac{ck}{2} + \beta(kU_0 + \lambda w\theta) + \ln\theta + (k-1) \times \ln\left[1 - \frac{(k-1)}{k}\theta\right] - k\ln(1-\theta). \quad (36)$$

Several conclusions can be drawn from the study in Fig. 2 (and data not shown for honeycomb and triangular lattices):

Table 1
Table of parameters used in the fitting of simulation data.

	Adsorbate	Geometry	$m(c,k)$	a	$g = mk$(AASI)	Fitted g	ε_g %
Fig. 1	Dimers ($k=2$)	$c=3$	3/2	1/3	3	2.906(2)	3.13
Fig. 2	Dimers ($k=2$)	$c=4$	2	1/4	4	3.790(8)	5.25
Fig. 3	Dimers ($k=2$)	$c=6$	3	1/6	6	5.560(6)	7.33

(1) In all cases, an excellent agreement is obtained between theoretical and simulation data. In other words, there exists a wide range of βw's, where the new theoretical framework provides an excellent fit to the simulation data. This finding is very important because (i) most of the experiments in surface science are carried out in this range of interaction energy, and (ii) the range studied includes values of βw's in the vicinity of the critical regime, where the disagreement between standard mean-field approximations and simulation data turns out to be significantly large (see insets in Fig. 2).

(2) The values of g calculated by fitting are very close to that predicted by AASI (see Table 1). Consequently, very small deviations appear between solid and dashed lines. Even though there exist similarities between the behavior of the system for the different geometries, the differences between fitted and theoretical values of g increase as the connectivity increases. These differences can be much easily quantified with the help of the percentage error, $\varepsilon_g\% = 100.\left|\frac{g_{fitted}-g_{theor}}{g_{theor}}\right|$, which takes the values of 3.13%, 5.25%, and 7.33% for honeycomb, square and triangular lattices, respectively. The explanation of this effect is simple: the value of g obtained from AASI overestimates the number of excluded states because of simultaneous exclusion of neighboring particles and this simultaneous exclusion increases as the number of neighbors increases. Note that $\varepsilon_g\% = 0$ for $c = 2$, given that for rigid k-mers adsorbed on one-dimensional lattices, it is straightforward to show that $m = 1$, and $g = k$, yields the exact adsorption isotherm obtained independently in Ref. [23].

(3) An unique value of g provides the best fit in the whole range of βw's. Then, once this value is obtained by fitting the adsorption isotherm for $\beta w = 0$, the rest of the adsorption isotherms (for $\beta w \neq 0$) are calculated without any adjustable parameters. The procedure demonstrates that an accurate description of the coverage and temperature dependence of the free energy of non-interacting k-mers and the use of the quasi-chemical approximation lead to a precise determination of the main adsorption properties of interacting polyatomics.

(4) The differences between MC simulation and MFA are very appreciable. In addition, the simplest approximation within FSTA, namely $g =$ constant, provides results comparable to those obtained with the scheme presented in Ref. [21]. These findings (i) show that the present approach represents a qualitative advance in the description of the adsorption k-mers with respect to the existing theories based on MFA; and (ii) suggest the potentiality of the model proposed in supporting the interpretation of experimental data of polyatomics species of different shape and size, beyond of the rigid linear molecules studied in Ref. [21].

Next, we compare our results to experimental data. For this purpose, experimental adsorption isotherms of propane in 13X zeolites [35] were examined in terms of the new isotherm function. In our analysis, Eqs. (28) and (31) were used assuming AASI. In addition, given that the analyzed experimental isotherms were reported in adsorbed amount v, against pressure p, we rewrite the variables in Eqs. (28) and (31) in a more convenient form. Thus, where $\theta = v/v_m, \beta\mu = \ln(p/p_0)$ and $K(T) = K_\infty \exp(-\beta H_{st}), H_{st}$ being the isosteric heat of adsorption.

For small molecules adsorbed in zeolites, the use of a two-dimensional lattice is widely accepted. As an example, this hypothesis is strongly supported by detailed simulations on zeolites 5A, where density profiles of O_2 and N_2 along the cavity radius show sharp peaks close to the wall [36]. On the other hand, an alkane chain can be considered as a "bead segment", in which each methyl group is represented as a single site (bead) [37]. In this frame, propane would correspond to $k = 3$. In addition, (i) the length of propane (6.7 Å) is relatively large with respect to the diameter of the cavity of a zeolite 13X (11.6 Å); and (ii) previous work indicates that 5–6 molecules can be adsorbed per cavity [35]. These findings suggest that the molecules should adsorb aligned along a preferential direction (otherwise, 5–6 molecules would hardly fit in the cavity).

The cases described in the paragraph above are some examples out of a whole variety of adsorption configurations that the proposed formalism allows to deal with. In the first case, the gas is adsorbed principally on the cavity walls forming a two-dimensional phase with $c/2$ possible orientations and this would correspond to $g = ck/2(m = c/2)$. In the case studied here, the calculation of the properties of the aligned state reduces to the calculation of a one-dimensional problem and, consequently, the exclusion parameter g is chosen equal to 3 ($k = 3$ and $m = 1$).

With respect to the energies involved in the adsorption process, and according to previous studies [8], we fix $H_{st} = -6.94$ kcal/mol and $w = -0.7$ kcal/mol. Then, we determine, by multiple fitting, the value of v_m leading to the best fit to the experimental data of C_3H_8/13X from Ref. [35] in the whole pressure and temperature range. The results are shown in Fig. 3 and the values of the parameters used in the fitting are collected in Table 2. Lines correspond to the present theory and symbols represent experimental data from [35]. The agreement between experimental and theoretical data is very good. In addition, as in the experiment, the resulting value of the monolayer volume, $v_m = 5.45$ molecules/cavity, is smaller than six molecules per cavity and the fractional value of v_m is indicative that some molecules may stand across the cavity's windows.

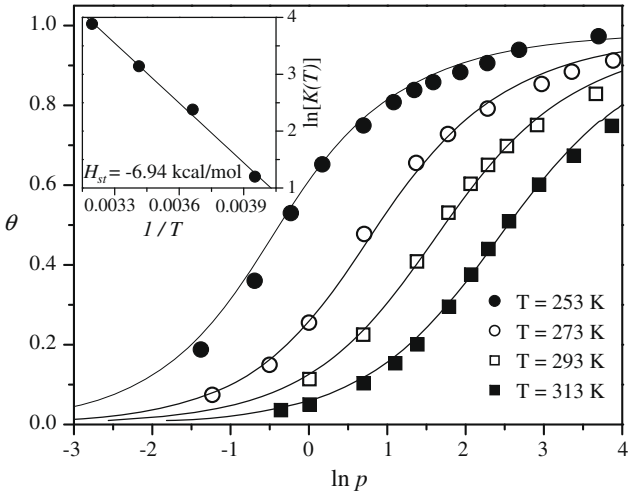

Fig. 3. Comparison between the theoretical model [Eqs. (28) and (31)] and experimental adsorption isotherms for C_3H_8 adsorbed in 13X zeolite [35]. The symbols and lines correspond to experimental data and the present theory, respectively. Inset: temperature dependence of the equilibrium constants used in the fitting process. The slope of the curve corresponds to the isosteric heat of adsorption.

Table 2
Table of parameters used in the fitting of experimental data.

System	k	m	g	v_m (molecules/cavity)	H_{st} (kcal/mol)	w (kcal/mol)
C_3H_8/13X	3	1	3	5.45	−6.94	−0.7

This comparison with a set of experimental results provides just an example of the scope of this theory, which considers simply the cavities of the 13X zeolite as a linear array of adsorptive sites, the propane molecule as three bead units, and the lateral coupling as a constant interaction energy between two nearest-neighbor units belonging to different k-mers. Despite the present result, further research is clearly needed in order to conclusively evaluate the reliability and accuracy of this approach. However, note that a rather artificial model with eight fitting parameters was necessary to interpret analogous data in Ref. [35].

4. Conclusions

In the present paper, an analytical approach to the adsorption of interacting polyatomic adsorbates (k-mers) has been proposed. The new formalism was obtained by combining (i) the recently reported fractional statistics thermodynamic theory of adsorption of polyatomics, and (ii) a generalization of the classical QCA in which the adsorbate can occupy more than one adsorption site.

The proposed model is simple, easy to apply in practice, and provides an accurate description of the adsorption of interacting polyatomics. Physically, these advantages are a consequence of properly considering (i) the configurational entropy of the adsorbate and (ii) the lateral interactions in the adlayer. This treatment bears theoretical interest because it represents a qualitative advance with respect to the existing models of multisite-occupancy adsorption.

The new theory was compared with Monte Carlo simulation and analytical results from the classical Bragg-Williams approximation. Two main conclusions can be drawn from the comparison: (1) the theory is greatly improved by introducing the lateral interactions by following the configuration-counting procedure of the QCA; and (2) appreciable differences can be seen between BWA and the theory introduced here, with the last being the most accurate for all cases.

Finally, experimental data of C_3H_8 adsorbed in 13X zeolite were very well fitted by using the new model. Even though further comprehensive analysis of experimental isotherms needs to be done, the new theory seems to be a promising approach toward a more accurate description of the adsorption thermodynamics of interacting polyatomic molecules.

Acknowledgement

This work was supported in part by CONICET (Argentina) under Project PIP 6294; Universidad Nacional de San Luis (Argentina) under Project 322000 and the National Agency of Scientific and Technological Promotion (Argentina) under Project 33328 PICT 2005.

References

[1] W. Rudziński, D.H. Everett, Adsorption of Gases on Heterogeneous Surfaces, Academic Press, London, 1992.
[2] T. Nitta, M. Kuro-oka, T. Katayama, J. Chem. Eng. Jpn. 17 (1984) 45.
[3] T. Nitta, A.J. Yamaguchi, J. Chem. Eng. Jpn. 25 (1992) 420.
[4] A.W. Marczewski, A. Derylo-Marczewska, M. Jaroniec, J. Colloid Interface Sci. 109 (1986) 310.
[5] J.L. Riccardo, F. Romá, A.J. Ramirez-Pastor, Int. J. Mod. Phys. B 20 (2006) 4709.
[6] F.D.M. Haldane, Phys. Rev. Lett. 67 (1991) 937.
[7] Y.S. Wu, Phys. Rev. Lett. 73 (1994) 922.
[8] J.L. Riccardo, F. Romá, A.J. Ramirez-Pastor, Phys. Rev. Lett. 93 (2004) 186101.
[9] J.L. Riccardo, F. Romá, A.J. Ramirez-Pastor, Appl. Surf. Sci. 252 (2005) 505.
[10] F. Romá, J.L. Riccardo, A.J. Ramirez-Pastor, Ind. Eng. Chem. Res. 45 (2006) 2046.
[11] K.R. Paserba, A.J. Gellman, Phys. Rev. Lett. 86 (2001) 4338.
[12] K.R. Paserba, A.J. Gellman, J. Chem. Phys. 115 (2001) 6737.
[13] A.J. Gellman, K.R. Paserba, J. Phys. Chem. B 106 (2002) 13231.
[14] A.J. Phares, F.J. Wunderlich, J. D Curley, D.W. Grumbine Jr., J. Phys. A: Math. Gen. 26 (1993) 6847.
[15] A.J. Ramirez-Pastor, J.L. Riccardo, V. Pereyra, Surf. Sci. 411 (1998) 294.
[16] J.E. González, A.J. Ramirez-Pastor, V. Pereyra, Langmuir 17 (2001) 6974.
[17] F. Romá, A.J. Ramirez-Pastor, J.L. Riccardo, Phys. Rev. B 72 (2005) 035444.
[18] F. Romá, J.L. Riccardo, A.J. Ramirez-Pastor, Phys. Rev. B 77 (2008) 195401.
[19] P.M. Pasinetti, F. Romá, J.L. Riccardo, A.J. Ramirez-Pastor, Phys. Rev. B 74 (2006) 155418.
[20] T.L. Hill, An Introduction to Statistical Thermodynamics, Addison Wesley Publishing Company, Reading, MA, 1960.
[21] M. Dávila, F. Romá, J.L. Riccardo, A.J. Ramirez-Pastor, Surf. Sci. 600 (2006) 2011.
[22] F. Romá, J.L. Riccardo, A.J. Ramirez-Pastor, Langmuir 22 (2006) 3192.
[23] A.J. Ramirez-Pastor, T.P. Eggarter, V. Pereyra, J.L. Riccardo, Phys. Rev. B 59 (1999) 11027.
[24] P.J. Flory, J. Chem. Phys. 10 (1942) 51;
P.J. Flory, Principles of Polymer Chemistry, Cornell University Press, NY, Cornell, 1953.
[25] M.L. Huggins, J. Chem. Phys. 46 (1942) 151;
M.L. Huggins, Ann. NY Acad. Sci. 41 (1942) 151;
M.L. Huggins, J. Am. Chem. Soc. 64 (1942) 1712.
[26] E.A. Guggenheim, Proc. Royal Soc. London A183 (1944) 203.
[27] E.A. DiMarzio, J. Chem. Phys. 35 (1961) 658.
[28] K. Binder (Ed.), Monte Carlo Methods in Statistical Physics, Topics in Current Physics, vol. 7, Springer, Berlin, 1978.
[29] D. Nicholson, N.D. Parsonage, Computer Simulation and the Statistical Mechanics of Adsorption, Academic Press, London, 1982.
[30] K. Binder (Ed.), Applications of the Monte Carlo method in statistical physics, Topics in Current Physics, vol. 36, Springer, Berlin, 1984.
[31] N. Metropolis, A. W Rosenbluth, M.N. Rosenbluth, A.H. Teller, E. Teller, J. Chem. Phys. 21 (1953) 1087.
[32] A. Clark, The Theory of Adsorption and Catalysis, Academic Press, New York and London, 1970.
[33] A. Patrykiejew, S. Sokolowski, K. Binder, Surf. Sci. Rep. 37 (2000) 207.
[34] A.J. Ramirez-Pastor, J.L. Riccardo, V. Pereyra, Langmuir 16 (2000) 10167.
[35] M. Tarek, R. Kahn, E. Cohen de Lara, Zeolites 15 (1995) 67, and references therein.
[36] D. Razmus, C. Hall, AIChE J. 37 (1991) 769.
[37] L.J. Gallego, C. Rey, M.J. Grimson, Mol. Phys. 74 (1991) 383.